Detecting disturbance of uniformity of a nitrogen and CO_2 mixture in an acoustic tube

Leszek Remiorz*

Silesian University of Technology, Konarskiego 18, 44-100 Gliwice, Poland

Abstract

In light of concerns over climate changes, extensive scientific research is ongoing in the field of CO_2 separation [1–5]. No definitive determination has yet been made as to which separation technology should be selected and efforts are continuing to find new methods [6–11]. This paper presents preliminary results of measurements of the disturbance of the uniformity of a nitrogen and CO_2 mixture inside a thermoacoustic tube. Transversely to the tube axis, a detection path was placed to identify disturbance of the CO_2 and nitrogen content. The tube was filled with a uniform mixture of nitrogen and CO_2. An acoustic standing wave was induced inside the tube and the readings of the mixture uniformity disturbance detection system were recorded. More data were recorded from an internal microphone, enabling detection of the standing wave. The results were processed numerically and the computations resulted in a series of curves in the time and frequency domains, illustrating the behavior of the mixture inside the tube.

Keywords: CO_2 separation, CO_2 measurement, Acoustic separation

1. Introduction

Numerical calculations concerning the process of the impact of the acoustic wave on the uniformity of the nitrogen and CO_2 mixture indicate that, apart from the rapidly changing disturbance of the mixture uniformity which is synchronous with the forcing wave frequency, another slow-changing process takes place in the acoustic tube, causing uniformity disturbance related to the geometrical location of the analyzed point inside the tube [12, 13]. The measurements performed aim to provide experimental results to confirm this thesis.

The concept of the measuring stand is presented in Fig. 1. The basic element of the stand is a round

---
*Corresponding author

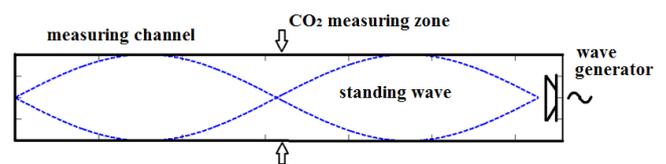*Email address:* leszek.remiorz@polsl.pl (Leszek Remiorz*)

Figure 1: Concept of the measuring stand

tube in which acoustic standing waves are generated. Transversely to the tube, a measuring path was placed to determine CO_2 concentration (marked with arrows in Fig. 1).

The investigations center on separating frequency ranges from the measuring signal, recorded by the CO_2 detector, which are not caused by acoustic forcing, the operation of the measuring system itself or by other interfering signals. These interfering signals include the power network frequency, the CO_2 detec-

tion path keying frequency, as well as the acoustic forcing frequency and all other frequencies higher than that. Attention should also be drawn to the fact that detection of frequencies lower than the forcing frequency would not only confirm that a slow-changing separation process was taking place but would also remove any doubts as to whether or not the recorded changes were caused by changes in the CO_2 partial pressure. A change in CO_2 partial pressure occurs with the frequency of acoustic excitations (the inductor oscillation frequency). In light of the above, it seems that detection of the slow-changing components in the measuring signal may be related exclusively to changes in the CO_2 content in the mixture. The measurements were made using atmospheric air for measurements "without CO_2", and a nitrogen and CO_2 mixture for measurements "with CO_2". The CO_2-nitrogen mixture, not the CO_2-air mixture, was selected so as to eliminate the possible impact of a third gas (oxygen).
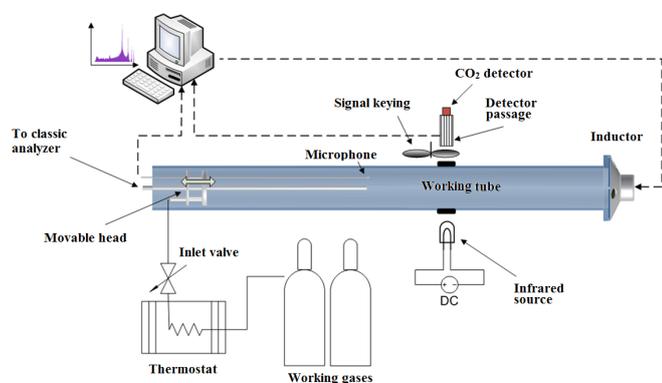
2. The test stand

Figure 2: Diagram of the test stand for the analysis of carbon dioxide separation

The diagram of the test stand for the analysis of the acoustic wave impact on the air and CO_2 mixture is shown in Fig. 2.

The measuring path was designed so that the system could operate in two modes, i.e. with and without keying. The principle of no-keying measurement takes advantage of the differential properties of the path of the measuring signal electronic processing. In the case of changes in the flux of light
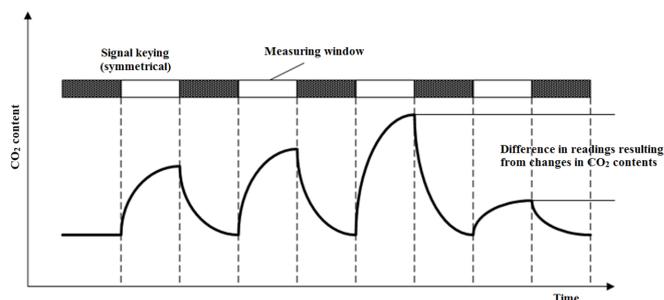

Figure 3: Curve illustrating the measuring signal with keying

falling on a photosensitive element of the CO_2 detector, the differential system generates an appropriate output signal dependent on the rate at which changes in the light flux illuminating the detector occur. The light flux illuminating the detector is constant so the changes in the lighting intensity result exclusively from changes in CO_2 concentrations along the measuring path. Because sensitivity of this method diminishes as the pulsation frequency of the light flux illuminating the measuring detector gets smaller, the method was used in the presented testing only as an auxiliary one. The other measuring method additionally takes advantage of the system of the measuring path keying (obscuring) with a constant pre-set frequency. The essence of the measurement is presented in Fig. 3. The measurement result is found in a short time interval determined by the keying frequency. After the measuring window is revealed (illuminated detector), the measuring signal intensity rises abruptly until the measuring window is obscured. The slope of the measuring signal curve depends on the intensity of the CO_2 detector illumination. Because the measuring window width is constant, the signal level will depend on the rate at which its intensity rises and, thereby, on the CO_2 concentration along the measuring path.

The real curve of the signal recorded in the measuring tube is presented in Fig. 4. Fig. 5 shows an enlarged fragment of the curve. Fig. 4a and Fig. 5a illustrate the excitation signal recorded by the measuring microphone inside the acoustic tube. This signal represents not only the acoustic forcing but also some unfavorable acoustic phenomena inside the tube, such as inside reflections off the tube and necessary structural elements (e.g. the gas supply connector pipe, etc.). The values of the applied
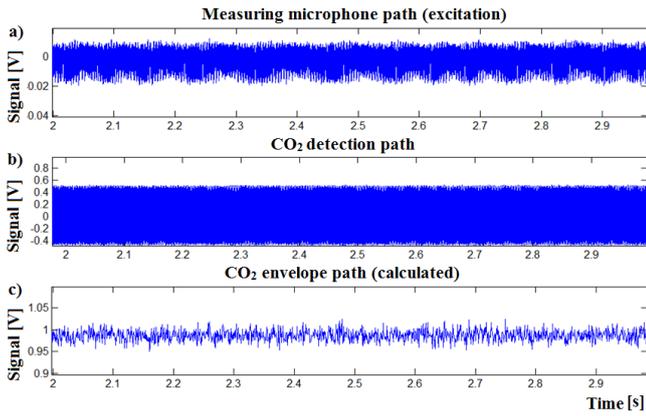
Figure 4: Curves illustrating the real measuring signal: a) measuring microphone path, b) CO_2 detection path c) calculated tube
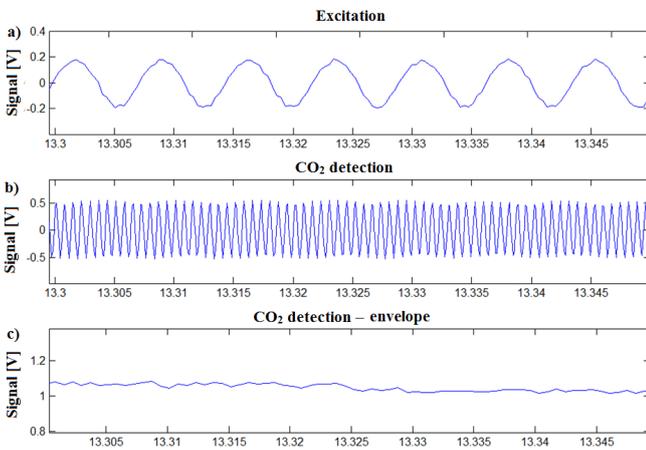

Figure 5: Example of a fragment of the curve in a short time window: a) measuring microphone path, b) CO_2 detection path, c) calculated tube—difference between maximum and minimum values for each cycle

acoustic forcing frequencies were included in the range of 80 Hz to 1 kHz.

3. Qualitative analysis of measurement data

Many cycles were recorded during the measurements. However, their unequivocal evaluation was burdened with high uncertainty. This resulted from the imperfections of the measuring device structure, including the temperature drift of the electronic elements, unsteady operation of the keying system, the hum of the power network, etc. In order to reduce the uncertainty of the measurement evaluation, a comparative method was used which con-
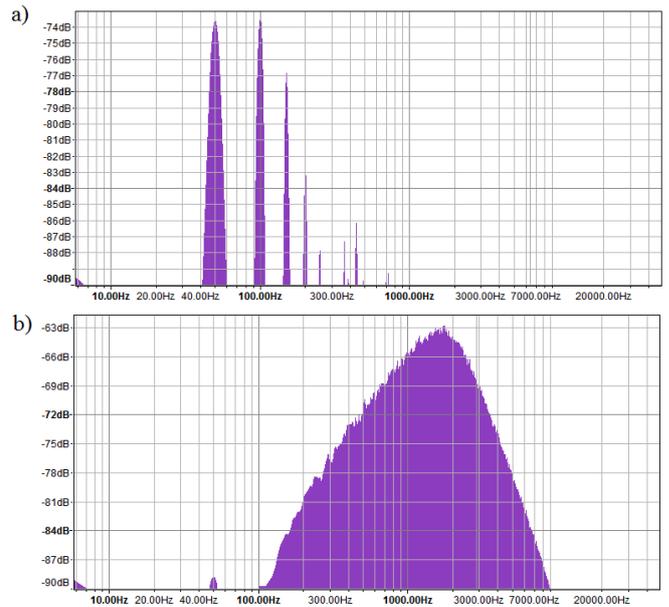

Figure 6: FFT analysis of curves plotted for the incomplete configuration: a) curve recorded by the measuring microphone, b) curve recorded for the CO_2 detection system
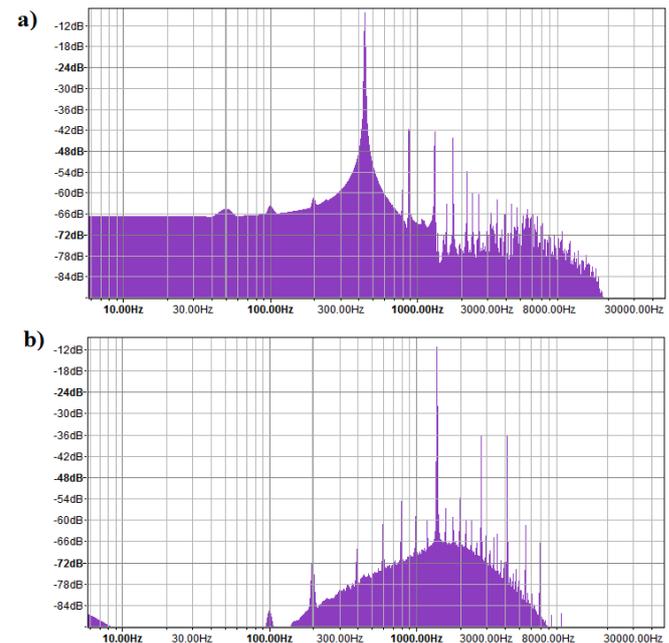

Figure 7: FFT analysis of the complete configuration curve: a) measuring microphone path, b) CO_2 detector path

sisted in classifying the measuring sessions into two measuring groups, i.e. the "incomplete configuration" and "complete configuration". The curves illustrating changes in the incomplete configuration were deprived of one of the key elements which obviously prevent the occurrence of the sought slow-

changing processes, i.e. there was no CO_2 in the acoustic tube or no acoustic excitation. The complete configuration measuring curves were plotted with all necessary factors present so that the slow-changing wave could be generated (if the phenomenon occurred). Two measuring curves were selected to be analyzed—plotted for the incomplete and complete configuration, respectively. The curve recorded for the incomplete configuration was deprived of the acoustic excitation and signal keying. A fragment of the curve illustrating the incomplete configuration under analysis is shown in Fig. 5. Fig. 5a illustrates the signal recorded by the measuring microphone, Fig. 5b—the signal from the CO_2 detection system. The results of the Fast Fourier Transform (FFT) analyses for the selected signals are presented in Fig. 6a and 6b, respectively. Both recorded signals have a very small amplitude compared to the complete configuration signal (Fig. 7)—at a level below 0.02 V. The FFT analysis reveals the system internal noise as well as the mains hum at the level of 50 Hz and with multiple frequencies Fig. 6a. The internal noise of the CO_2 detection path is also characteristic (Fig. 6b). It results from internal noise of individual components of the measuring system, as well as from the CO_2 detector temperature noise. The maximum amplitude of the noise coincides with frequencies of ~2 kHz and is at the level of -63 dB. The frequency of the arising noise is an essential parameter. Its value is by orders of magnitude higher than the value of the sought measuring signals, which makes it possible to remove this interference easily by means of filtering algorithms.

The measuring curves plotted for the complete configuration, i.e. with CO_2 present in the tube and with keying in progress, under acoustic excitation, are characterized by much higher amplitudes (Fig. 7a, 7b)—at the level of 0.5 V. It should be emphasized that the presented evaluation is a qualitative one and in this case quantitative relationships are ignored. For this reason, the signals are processed in the source form, i.e. in electric voltage units. The results of the measuring microphone path FFT analysis are presented in Fig. 7a.
The identified excitation frequency generating the mixture oscillation is 450 Hz (Fig. 7a). Higher frequencies visible in the chart result from the opera-

tion of the measuring path itself, as well as from the acoustic wave reflections inside the tube, and they are irrelevant to the process under consideration. The CO_2 detector measuring path analysis (Fig. 7b) indicates a strong signal with a frequency of about 1700 Hz. This is the measuring path keying frequency. No characteristic values were identified for sought frequencies below 100 Hz.

This may prove that there are no slow-changing processes. However, it has to be remembered that the FFT analysis tool has certain limitations, such as the loss of relation to time or—in particular—inaccuracy of results obtained in the case of transient signals.
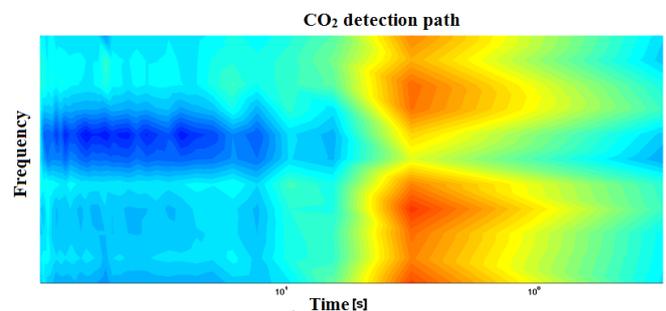

Figure 8: STFT analysis of the complete configuration process

Therefore, the measuring signals were additionally processed numerically. In order to identify the curves that could indicate an instantaneous separation of the mixture, the Short-Time Fourier Transform (STFT) analysis was conducted for the curve recorded by the CO_2 detector with a low-pass filter eliminating any frequencies higher than the mixture excitation frequency. The effect of numerical processing is the image presented in Fig. 8. The areas in red point to the occurrence of frequencies higher than 1 Hz. This may prove the occurrence of a low-frequency wave (Fig. 8).

In order to obtain clearer results, a data processing method should be applied that is more suitable for the recorded curves. The wavelet decomposition of the signal seems appropriate. Daubechies wavelets were used for the analysis [14]. The source signals come from tubes calculated as the incomplete and complete configuration. The aim of the wavelet decomposition is to separate anticipated slow-changing signals confirming the conjecture that the acoustic wave disturbs the uniformity of the air and CO_2 mixture.
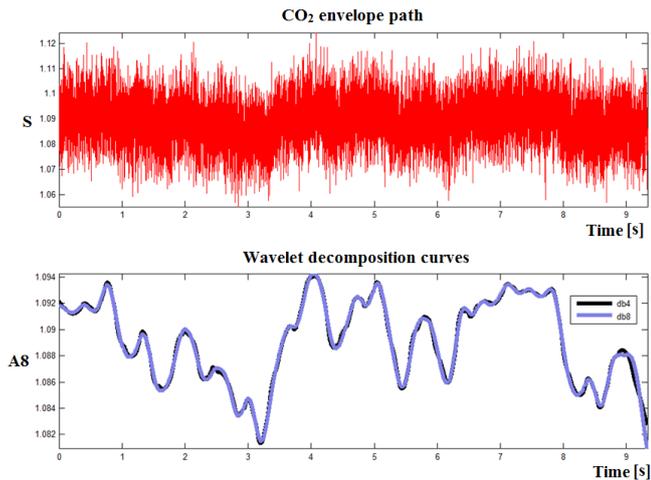
Figure 9: Complete configuration curve after decomposition using db4 and db8 wavelets

The calculations were performed using two kinds of wavelets, marked as db4 and db8. Fig. 9 presents the result of the measuring signal wavelet decomposition using db4 and db8 wavelets. In both cases the presented curves are almost identical, which makes it possible to believe that the calculations are correct.
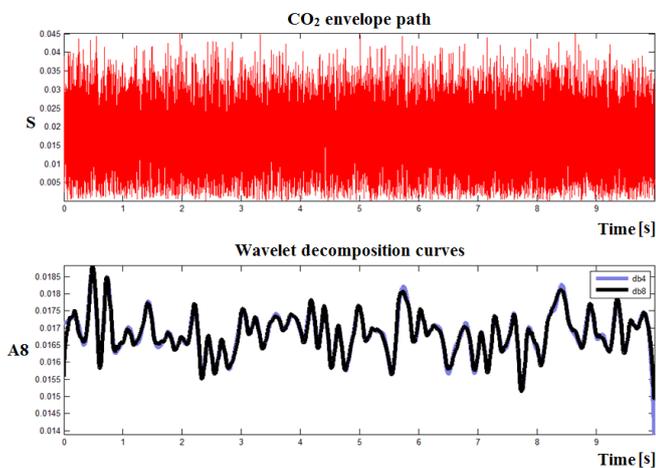

Figure 10: Incomplete configuration curve after decomposition using db4 and db8 wavelets

The incomplete configuration curve was analyzed in the same manner (Fig. 10). The curves obtained as a result of decomposition using db4 and db8 wavelets were very similar. Comparing the charts for the signal in the complete and incomplete configuration, it should be concluded that the curves plotted for the former are characterized by much higher amplitudes.

The amplitude maximum difference for the curve plotted for the incomplete configuration is 0.003, in relative units; for the complete configuration it is almost five times higher: 0.014, which proves that cases of instantaneous disturbance of the air and CO_2 mixture arise due to the acoustic wave impact.

4. Conclusions

The performed measurements are not irrefutable evidence of the occurrence of slow-changing processes disturbing the uniformity of the nitrogen and CO_2 mixture in an acoustic tube. However, analyzing the measurement results presented in this paper, it can be noticed that such a process may actually occur. It is especially evident if the measurement results are compared in two groups. The first group includes measurements performed for the incomplete configuration; the second—for the complete measuring configuration. The "incomplete configuration" is understood as a system which is deprived of at least one of the elements creating the conditions for the analyzed phenomenon to arise, i.e. without acoustic excitation with other measuring systems operating and/or without CO_2 in the acoustic tube under acoustic excitation.

It should be noted that the acoustic tube treated as a "no CO_2 tube" also included small amounts of CO_2 contained in atmospheric air.

On the other hand, the amplitude of the curves illustrating slow-changing processes for the complete configuration is substantially higher, which indirectly indicates that the analyzed process does occur in the acoustic tube.

References

[1] A. Skorek-Osikowska, J. Kotowicz, K. Janusz-Szymańska, Comparison of the energy intensity of

the selected CO_2-capture methods applied in the ultra-supercritical coal-fired power plants, Energy & Fuels 2012.

[2] G. Wiciak, J. Kotowicz, Experimental stand for CO_2 membrane separation, Journal of Power Technologies 91 (4) (2011) 171–178.

[3] . Bartela, A. Skorek-Osikowska, J. Kotowicz, Integracja bloku elektrociepłowni węglowej na parametry nadkrytyczne z instalacją wychwytu dwutlenku węgla oraz turbiną gazową [integration of a supercritical coal-fired combined heat and power plant unit with a carbon dioxide capture installation and a gas turbine], Rynek Energii 3(100) (2012) 56–62.

[4] G. Wiciak, Identyfikacja wybranych charakterystyk separacji CO_2 membrany kapilarnej polimerowej [identification of selected characteristics of CO_2 separation of the capillary polymer membrane], Rynek Energii 3(100) (2012) 94–100.

[5] K. Janusz-Szymańska, K. J., Analiza procesu membranowej separacji CO_2 w supernadkrytycznym bloku węglowym [analysis of the CO_2 membrane separation process in an ultra-supercritical coal-fired power unit], Rynek Energii 3(94) (2011) 53–56.

[6] D. Geller, G. Swift, Thermodynamic efficiency of thermoacoustic mixture separation, J. Acoust. Soc. Am. 112.

[7] T. Laurell, F. Petersson, A. Nilsson, Chip integrated strategies for acoustic separation and manipulation of cells and particles, Chem. Soc. Rev. 2007.

[8] D. R. Rector, M. S. Greenwood, A. Salahuddin, S. R. Doctor, G. J. Posakony, V. S. Stenkamp, Simulation of ultrasonic-driven gas separations, Acoustical Society of America.

[9] G. Swift, P. Spoor, Thermal diffusion and mixture separation in the acoustic boundary layer, J. Acoust. Soc. Am. 106.

[10] L. Remiorz, S. Dykas, S. Rulik, Numerical modelling of thermoacoustic phenomenon as contribution to thermoacoustic engine model, Task Quarterly 14 (3) 261–273.

[11] S. Rulik, L. Remiorz, S. Dykas, Application of the CFD technique for numerical modelling of the thermoacoustic engine, Archives of Thermodynamics 32 (3) (2011) 175–191.

[12] L. Remiorz, S. Rulik, S. Dykas, Numerical modelling of the CO_2 separation process, Archives of Thermodynamics 34 (1).

[13] L. Remiorz, Koncepcja wykorzystania fali termoakustycznej w procesie separacji CO_2 [a concept of the use of the thermoacoustic wave in the CO_2 separation process], Rynek Energii 4 (2012) 121–125.

[14] J. T. Białasiewicz, Falki i aproksymacje [Wavelets and approximations], WNT, Warszawa, 2000.

[15] P. Glynne-Jones, M. Hill, Acoustic manipulation combined with other force fields, Lab Chip 13 (2013) 1003.